

Wear Behaviour of Al_2O_3 –TiCN Composite Ceramic Sliding Against Pure Al, Fe and Stainless Steel

Zhao Xingzhong, Liu Jiajun, Zhu Baoliang, Luo Zhenbi & Miao Hezhou

Tribology Research Institute, Tsinghua University, Beijing, China

(Received 20 December 1995; accepted 19 March 1996)

Abstract: The sliding wear tests were carried out under dry friction conditions at ambient temperature on a block-on-ring tribometer in order to simulate the real cutting practice of ceramic cutting tools. The investigated materials include a composite ceramic Al_2O_3 –TiCN, Al, Fe and a stainless steel (AISI 302), which were combined into three ceramic/metal sliding pairs. The load and speed ranged from 98 to 294 N and from 0.30 to 0.78 m/s, respectively. The test results indicate that the wear of the three metals was much higher than that of the ceramic and Al showed the highest wear rate among them. The wear scars and wear debris were examined by a scanning electron microscope with an energy-dispersive X-ray spectroscopy analyser. The results showed that the metals were easily transferred on to the ceramic surface in the rubbing process, and the ceramic microfracture fragments were also embedded into metal surfaces. The wear mechanisms of both the ceramic and the metals were discussed in detail. © 1997 Elsevier Science Limited and Techna S.r.l. All rights reserved

1 INTRODUCTION

Ceramics, because of their excellent properties, such as high melting point, high hardness, good wear and corrosion resistance, antioxdation behaviour at high temperature, etc., have been widely used in many technical areas.^{1–3} The tribology of ceramics has developed rapidly in recent years and great progress has been achieved in this field.^{4–8}

Most of the reported results in recent years are involved in ceramic/ceramic pairs. The wear and friction information about ceramic/metal pairs is still relatively insufficient, which may be one of the major restricting factors for much wider use of ceramics in many possible technical areas. In this paper, the wear and friction behaviours of Al_2O_3 –TiCN ceramic sliding against three metallic materials under unlubricated conditions were evaluated on a block-on-ring testing machine, which could simulate a real cutting practice and provide some useful data for wear control of ceramic cutting tools. The wear surfaces were examined by a scan-

ning electron microscope with an energy-dispersive X-ray spectroscopy analyser, and the wear mechanisms were discussed.

2 EXPERIMENTAL METHOD

2.1 Wear test equipment and samples

The wear experiments were conducted on a block-on-ring testing machine. The contact model of the block and ring samples is shown in Fig. 1. The rotating speed of the machine could be adjusted from 0 to 400 rpm and the load could be changed from 0 to 1960 N. The ceramic block samples were produced by the Fine Ceramic Company of Tsinghua University. Their size was $5 \times 5 \times 20$ mm. The machined metallic ring samples were 40 mm in diameter and 10 mm in width. The frictional surface roughness of the blocks and the rings was $R_a = 0.32 \mu\text{m}$ and $R_a = 0.27 \mu\text{m}$, respectively. The main properties of the ceramic and the metallic materials are listed in Table 1.

Table 1. Properties of the experimental ceramic and metallic materials

Materials	Ceramic	Al	Fe	Stainless steel
Hardness	HRA94	HB45	HB177	HB187
Tensile strength ($\text{N}\cdot\text{mm}^{-2}$)	—	110	300	520
Density ($\text{g}\cdot\text{cm}^{-3}$)	5.12	2.73	7.80	7.90
Compositions	$\text{Al}_2\text{O}_3\cdot\text{TiCN}$	$\text{Al}(>99.5\%)$	$\text{Fe}(\text{C}<0.04\%)$	$\text{Ni}(9\%),\text{Cr}(18\%)$

2.2 Experimental procedure

Under unlubricated conditions and at ambient temperature, the wear behaviour of the ceramic/metal pairs was tested as a function of load and speed, respectively. The load range was 98–294 N, and the speed range was 0.30–0.78 m/s. The sliding time was 10 min for each pair after a 2 min running-in process. At least two tests were performed for every selected speed and load condition, and new specimens were used for each test. Before and after testing, the specimens were ultrasonically cleaned in an acetone bath for 15 min. The wear quantity of the block was calculated from its wear scar width, measured with an optical microscope.

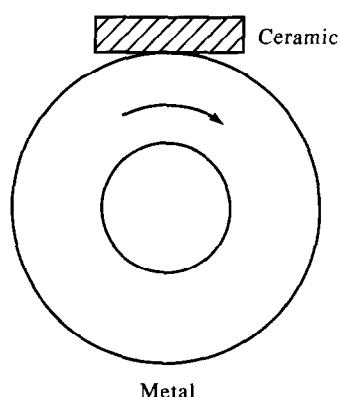
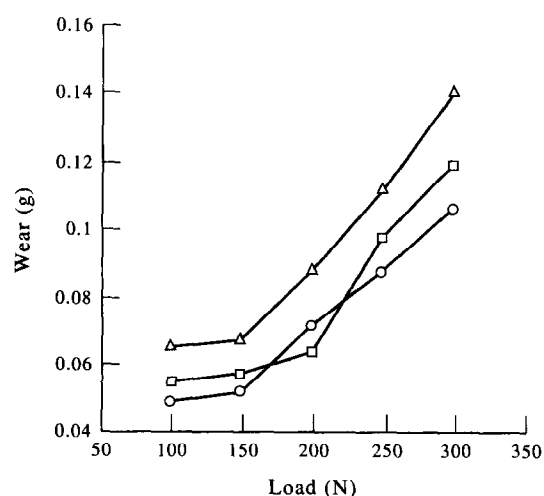
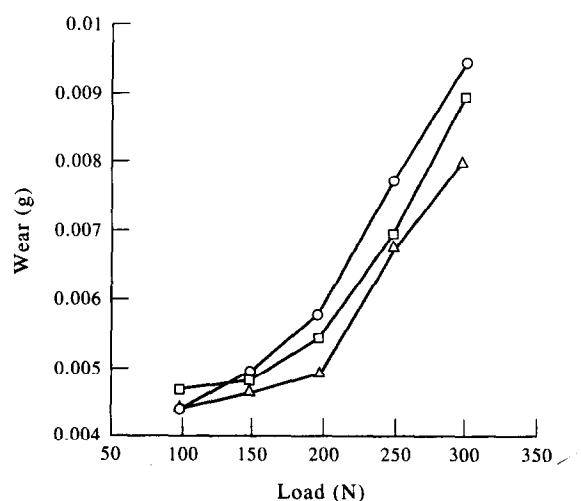


Fig. 1. Scheme of the contact model of block and ring.



(a)



(b)

Fig. 2. The variation of wear with load (speed 0.48 m/s): (a) for metals, \triangle — Al, \square — Fe, \circ — stainless steel; and (b) for ceramics, \triangle — against Al, \square — against Fe, \circ — against stainless steel.

The wear quantity of the ring samples was evaluated using a precision balance. The wear surface was examined by a scanning electron microscope with an energy-dispersive X-ray spectroscopy analyser.

3 RESULTS AND DISCUSSIONS

3.1 Effect of load on wear

The relationship between wear and load at a constant speed (0.48 m/s) is shown in Fig. 2(a) for the metallic samples and Fig. 2(b) for the ceramic samples. It could be seen that the wear increased gradually with load from 98 to 196 N. The steep increase in wear may be related to the transition of wear mechanism. In the lower load range (from 98 to 196 N), the main wear mechanisms of the metals may be abrasive wear and oxidation wear. In the high load range, the wear mechanisms of the metals may change into adhesive wear, and the ceramic wear was mainly caused by the adhesion of the rubbing surfaces and the microfracture of the ceramic. So the wear of both the metal and the ceramic was higher in the high load range. Figures 3(a) and 3(b) show the typical morphologies of the worn surfaces of the aluminium rings at a load of 98 N compared to that at 294 N. A lot of adhesive marks and scratching grooves can be seen on the worn surface formed at 294 N.

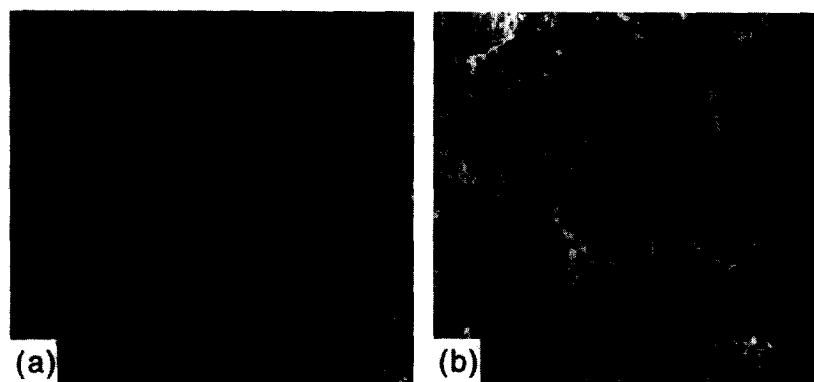


Fig. 3. SEM morphologies of worn Al surfaces ($\times 300$): (a) 98 N, 0.48 m/s; (b) 294 N, 0.48 m/s.

The wear quantity of the metals is more than 10 times larger than that of the ceramics, which is obviously due to the high hardness of the latter. Among the three metallic materials, Al has the lowest hardness, and has a stronger tendency to be oxidized in comparison to Fe and stainless steel, which makes it easily adhered to the ceramic ($\text{Al}_2\text{O}_3\text{--TiCN}$) surface. The metal transfer on to

the ceramic surface occurred for all three metals, but was different in magnitude due to the different properties of the metals. Figures 4(a) and 4(b) indicate the morphologies of the transfer films of Al and stainless steel under identical operating conditions. The lowest wear of the ceramic sliding against aluminium ring may be due to the following factors: (a) the transfer film of Al on the

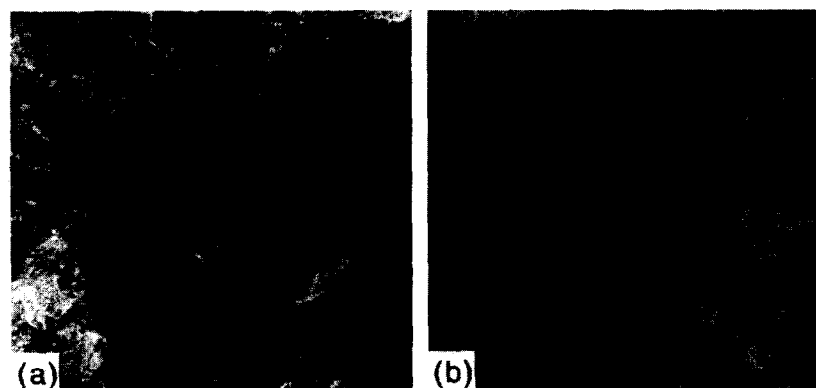


Fig. 4. SEM morphologies of metal transfer films on the ceramic surfaces ($\times 300$): (a) for Al, 196 N, 0.48 m/s; (b) for stainless steel, 196 N, 0.48 m/s.

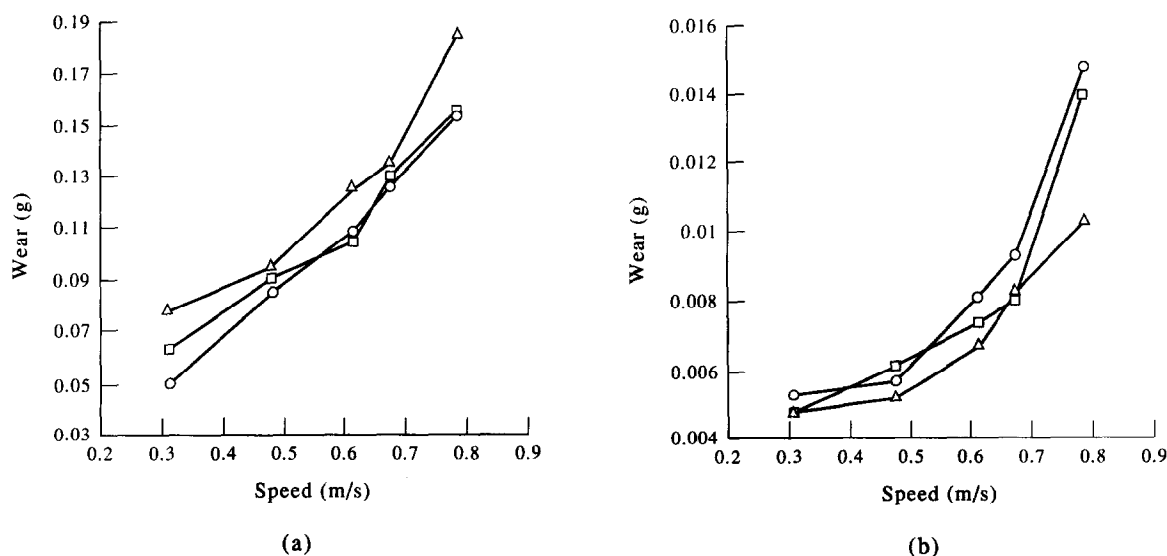


Fig. 5. The variation of wear with speed (load 196 N): (a) for metals, \triangle — Al, \square — Fe, \circ — stainless steel; and (b) for ceramics, \triangle — against Al, \square — against Fe, \circ — against stainless steel.

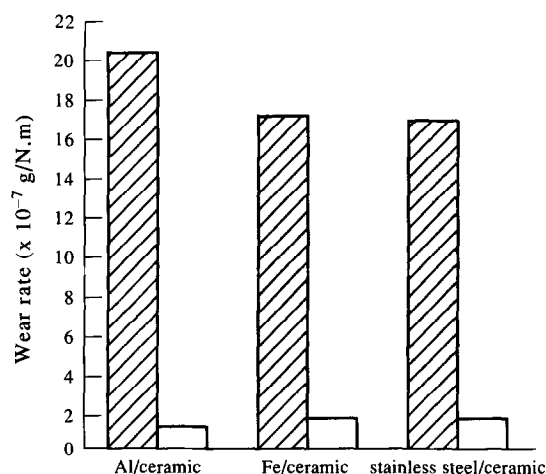


Fig. 6. Comparison of wear rates of the three ceramic/metal pairs.

ceramic surface is more complete than that of stainless steel, which can play a role in protecting the ceramic from wear to some extent; (b) Al is softer and causes lower stresses on the ceramic than the other metals do. Both these factors made the wear of the ceramic block rubbing against Al ring lower than against the other two metal rings.

3.2 Effect of speed on wear

Figure 5 shows the relationship between wear quantity and speed, at a load of 196 N. It indicates that the wear increased with the speed. At high speed, the intensive adhesion occurred between the ceramic and the metal, i.e. the adhesive wear predominated at these conditions because of the elevated temperature of the rubbing surfaces. Al showed the largest wear quantity due to its low melting point. The mean wear rates of these materials are shown in Fig. 6. The worn surfaces of Al at lower and higher speed are shown in Fig. 7.

3.3 Materials transfer between rubbing surfaces

The transfer film of metallic materials on the ceramic surfaces could be found after all tests (see Fig.

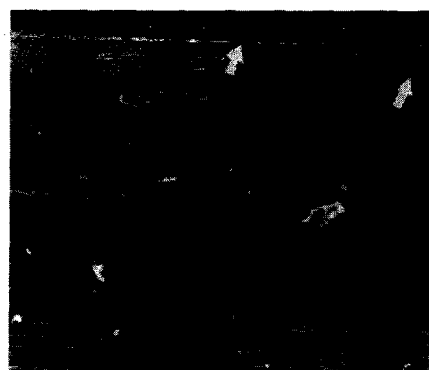


Fig. 8. SEM morphology of the worn stainless steel surface ($\times 300$), 196 N, 0.48 m/s.

4). Under the same conditions, the transfer amount of Al on the ceramic surface was much larger than that of Fe and stainless steel. The difference may be caused by the different hardness and oxidation activity of the metallic materials. Bowden and Tabor⁹ have studied the relationship of adhesive coefficient and hardness of many metals. They considered that the adhesive coefficients of metals decrease with increasing hardness, i.e. for the metals of low hardness, the adhesion can occur more easily than for those of high hardness. In addition, McDonald and Eberhalt¹⁰ thought that the adhesive tendency of metals to the surface of oxide ceramics (Al_2O_3 , ZrO_2 , etc.) is directly related to their oxidation activities — the more easily the metals are oxidized, the greater the adhesive forces between them and the oxide ceramic surfaces. The standard heats of formation of Fe_3O_4 and Al_2O_3 are -1117.9 kJ/mol and -1676.8 kJ/mol, respectively,¹¹ which indicates that Al is oxidized more easily than Fe, and can explain why the wear quantity of Al is greater than that of Fe and stainless steel.

Not only were the metallic materials transferred on to the ceramic surfaces in the rubbing process, but also the ceramic fracture fragments were embedded in the metal surfaces. The black points indicated by the arrows in Fig. 8 are ceramic fragments, and the X-ray energy dispersion spectrum is

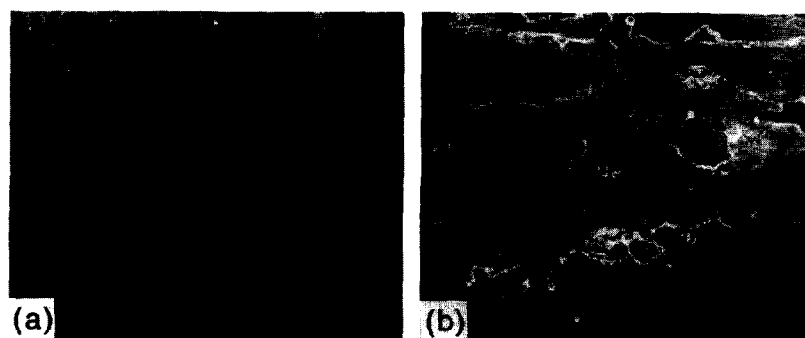


Fig. 7. SEM morphologies of worn Al surfaces ($\times 300$): (a) 196 N, 0.78 m/s; (b) 196 N, 0.30 m/s.

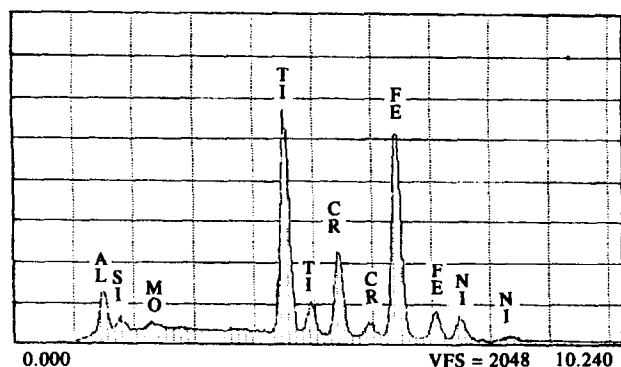
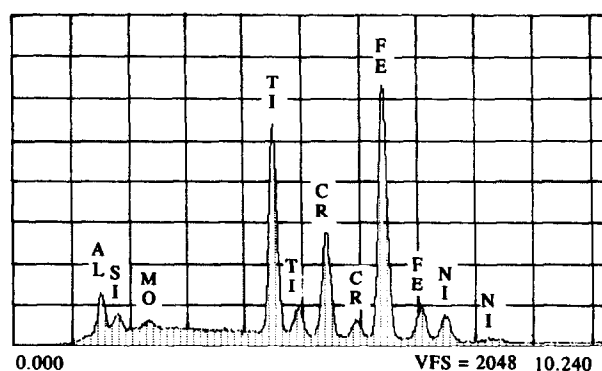
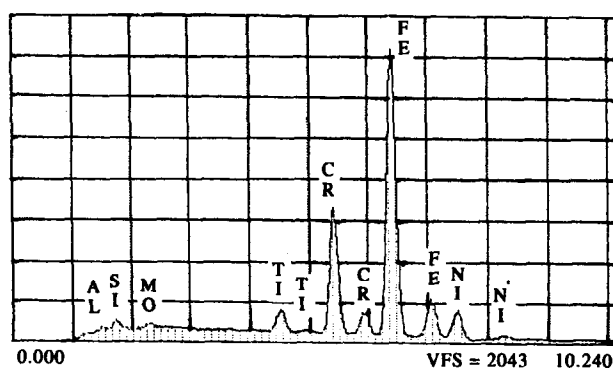


Fig. 9. X-ray energy dispersion spectrum of the embedded ceramic fragment.

shown in Fig. 9. The existence of Fe, Cr and Ni in Fig. 10(a) show the transfer of the stainless steel on the worn ceramic surface, while the Ti and Al peaks in Fig. 10(b) were brought about by the embedded ceramic fragments on the worn stainless steel surface. From the above, the wear mechanism of the ceramic could be described as Fig. 11.



(a)



(b)

Fig. 10. X-ray energy dispersion spectrum of the worn surfaces (a) for ceramic, and (b) for stainless steel.

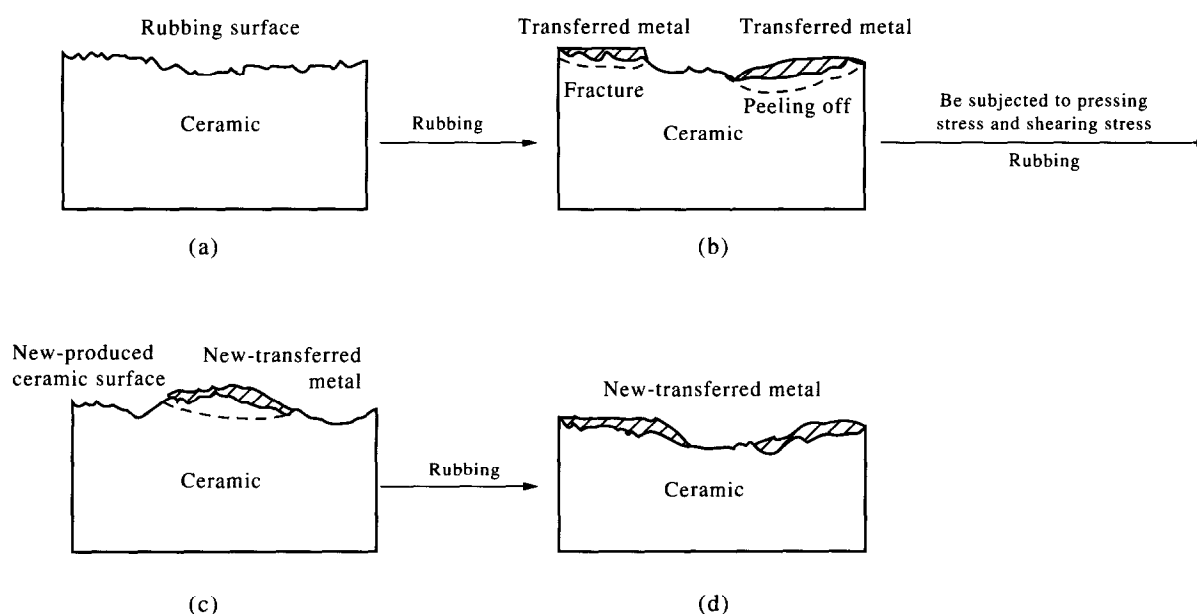


Fig. 11. Schematic description of the ceramic wear mechanisms.

4 CONCLUSIONS

The following conclusions can be drawn:

1. Under dry conditions, the wear quantity of both the ceramic and the metals increases rapidly with the load and speed for the ceramic/metal pairs. Adhesive wear predominates in the rubbing process.
2. Among the three metallic materials, namely Al, Fe and stainless steel, Al shows the strongest adhesive tendency to the ceramic surface because of its low hardness and high oxidation activity.
3. The wear quantity of the ceramic block is lowest when sliding against the Al ring. The relatively complete transfer film of Al on the ceramic surface plays a role in protecting the ceramic from wear, while the transfer films of Fe and stainless steel on the ceramic surfaces are not as complete as the Al film.

4. In the rubbing process, not only do the metals transfer on to the surfaces of the ceramics, but also microfracture fragments of the ceramics were embedded into the metal surfaces.

ACKNOWLEDGEMENT

The authors would like to thank the National Natural Science Foundation of China for their financial support to this research.

REFERENCES

1. LIU JIAJUN, *Wear Principle and Wear Resistance of Materials* (in Chinese). Tsinghua University Press, Beijing, 1993, pp. 270–282.
2. OU, BEMING, Tribology of ceramics. *Lubrication and Seal (in Chinese)*, **3** (1992) 63–68.
3. LIU, XIAOYU, Study on ceramic bearing materials. *Mech. Eng. Mater. (in Chinese)*, **4** (1984) 77–79.
4. WOYDT, M. & SCHWENZIEN, J., Dry and water-lubricated slip-rolling of Si_3N_4 - and SiC -based ceramics. *Tribol. Int.*, **26** (1993) 165–173.
5. SKOPP, A. & WOYDT, M., Ceramic-ceramic composite materials with improved friction and wear properties. *Tribol. Int.*, **25** (1992) 61–70.
6. TOMIZAWA, H. & FISCHER, T. E., Friction and wear of silicon nitride at 150–800 °C. *ASLE Trans.*, **29** (1986) 481–488.
7. TOMIZAWA, H. & FISCHER, T. E., Friction and wear of silicon nitride and silicon carbide in water: Hydrodynamic lubrication at low sliding speed obtained by tribochemical wear. *ASLE Trans.*, **30** (1987) 41–46.
8. KLAFKE, D., Fretting wear of ceramic-steel: The importance of wear ranking criteria. *Wear*, **104** (1985) 337–343.
9. BOWDEN, F. P. & TABOR, D., *The Friction and Lubrication of Solids, Parts 1 and 2*. Clarendon Press, Oxford, 1950 and 1964, pp. 299–314 and pp. 87–107.
10. McDONALD, J. E. & EBERHALT, J. G., Adhesion in aluminium oxide-metal systems. *Trans. Metall. Soc. AIME*, **233** (1965) 512–517.
11. HIRATSUKA, K., ENOMOTO, A. & SASADA, T., Friction and wear of Al_2O_3 , ZrO_2 and SiO_2 rubbing against pure metals. *Wear*, **153** (1992) 361–373.